Recent Progress in the Development of Solid Oxide Electrolyzers at ECN

J. P. Ouweltjes, L. Berkeveld, B. Rietveld

This document appeared in

Detlef Stolten, Thomas Grube (Eds.):
18th World Hydrogen Energy Conference 2010 - WHEC 2010
Parallel Sessions Book 3: Hydrogen Production Technologies - Part 2
Proceedings of the WHEC, May 16.-21. 2010, Essen
Schriften des Forschungszentrums Jülich / Energy & Environment, Vol. 78-3
Institute of Energy Research - Fuel Cells (IEF-3)
Forschungszentrum Jülich GmbH, Zentralbibliothek, Verlag, 2010
ISBN: 978-3-89336-653-8

Recent Progress in the Development of Solid Oxide Electrolyzers at ECN

Jan Pieter Ouweltjes, **Loek Berkeveld**, **Bert Rietveld**, Energy Research Centre of the Netherland (ECN), The Netherlands

1 Introduction

ECN has been active in the development of high-temperature electrolyzers since the year 2006. The experimental research has been focusing on the evaluation of different concepts for high-temperature electrolysis. The investigated cell designs were based on solid oxide fuel cell technology. From the experimental research it became clear that hydrogen electrode supported cells were potentially the preferred option, as the ohmic losses across the electrolyte were considerably lower than those obtained with electrolyte supported cells. The use of hydrogen electrode supported cells was however not straightforward. A potential drawback of using this cell technology was the occurrence of mass transport limitations in the porous mechanical support depending on its porosity and tortuosity, which limited the operating window with respect to feed gas composition and steam utilization [1]. Later, it was shown that the operating window was considerably improved by increasing the porosity of the 500 µm thick mechanical support from 30 to 40 vol%. The increased porosity allowed for operation at 70% steam utilization, yielding 93% electrical efficiency at 850°C. Operation at current densities higher than 0.5 Acm^{-2} was however still problematic [2].

In contrast to the difficulties encountered with hydrogen electrode supported cells, it became clear that electrolyte supported cells did not suffer from mass transport limitations. This allowed for electrolyzer operation at much higher current density than would be possible with hydrogen electrode supported cells. This is why ECN, as a partner in the European project RelHy, adopted electrolyte supported cell technology for operation at the targeted current density of 1 Acm^{-2}. This paper summarizes the achievements that were recently been obtained on electrolyte supported cells within the RelHy consortium.

2 Experimental

The aim of the experimental research was to develop an electrolyte supported electrolyzer cell that can be operated at 800°C, -1 Acm^{-2} current density and 60% steam utilization. The adopted electrolyte composition was $Sc_{0.20}Ce_{0.01}Zr_{0.79}O_{2-\delta}$ (10Sc1CeSZ), a ceramic oxide that exhibits considerably higher ionic conductivity than the yttria doped zirconias at 800°C [3]. The investigated electrolyte substrates were made by conventional tape casting. The 10Sc1CeSZ powder was purchased at Daiichi Kigenso Kagaku Kogyo Corporation, Japan. The powder was processed to slurry by mixing with a proprietary binder system, and ball milling was used for homogenization. The tape casting was done at two different blade heights in order to produce substrates with different thicknesses. After tape casting, the resulting tapes were cut to the right size, and sintered in air at 1400°C for 1 h. The size of the

electrolyte substrates was 108x108 mm^2. The resulting thicknesses were 115 and 215 µm, respectively.

The electrodes that were applied onto the electrolytes were deposited by means of screen printing and were 90x90 mm^2 in size. First, an approximately 5 µm thick layer of $Y_{0.2}Ce_{0.8}O_{2-\delta}$ (YDC, Praxair Specialty Ceramics) was applied at the oxygen electrode side of the electrolyte, and this layer was sintered at 1400°C 1 h. Next, the hydrogen electrode was applied. This electrode was composed of three layers. First, an approximately 5 µm thick layer consisting of $Gd_{0.4}Ce_{0.6}O_{2-\delta}$ (Praxair) was applied. On top of that an approximately 15 µm thick composite of 65 w% NiO and 35 w% $Gd_{0.1}Ce_{0.9}O_{2-\delta}$ (Praxair) was put. And finally, an approximately 20 µm thick layer of NiO (Mallinckrodt Baker) was put on top. The hydrogen electrode was then sintered at 1250°C for 1 h. Then, an approximately 70 µm thick $La_{0.6}Sr_{0.4}Co_{0.2}Fe_{0.8}O_{3-\delta}$ or LSCF (Praxair, including a heat treatment at 1100°C for 1 h) was applied on top of the YDC coating to act as oxygen electrode, and the assembly was given its final heat treatment at 1100°C for 1 h.

The prepared cells were tested in a test set-up that allowed for testing in both fuel cell mode and electrolyzer mode. The cell housing was made of dense alumina and included parallel flow channels in counter-flow arrangement. Current collection at the oxygen electrode was done by means of platinum mesh, and current collection at the hydrogen electrode was done with nickel mesh. The gas flows, including steam, were controlled by means of Bronkhorst flow controllers. The hydrogen electrode compartment of the cell housing was sealed by double layer gold/glass seal, which required heating to 1000°C prior to electrochemical testing to establish gas tightness. The glass bars were made of Schott G018-251 glass. In order to check for gas tightness of the hydrogen electrode compartment, the exhaust flow rate of the hydrogen electrode was measured. This was done by means of a gas flow meter (Bronkhorst), after drying the exhaust flow of the hydrogen electrode exhaust by Peltier cooling. The applied clamping force during the experiments was 0.2 $kgcm^{-2}$ for all test cells. This was achieved by putting weights on a spindle that rested on top of the cell housing. DC electrical loading was established with a Kikusui PLZ1004W in conjunction with a Delta Elektronika SM15-200D power supply. The cell voltage was recorded by means of a Keithley voltmeter. Electrochemical impedance spectroscopy measurements were performed with a Gamry FC500 potentiostat between 100 kHz and 0.1 Hz. The used AC amplitude varied with DC load; until 20 A DC load, an amplitude of 1 A was used, between 20 and 60 A DC load, the amplitude was 2 A, and above 60 A DC load, the amplitude was increased to 3 A. The obtained impedance spectra were fitted to an equivalent circuit using the computer program Echem Analyst.

The procedure followed during the cell tests comprised the following steps:

- Heating to 1000°C cell temperature with a 30°C h^{-1} ramp and 2 h dwell time, and followed by cooling to 800°C, while feeding the hydrogen electrode with 1000 ml min^{-1} nitrogen and feeding the oxygen electrode with N_2-O_2 80-20vol%
- Reduction of the hydrogen electrode by stepwise replacing the nitrogen flow with H_2-4%H_2O
- Cell operation in fuel cell mode during 24 h at 1 A cm^{-2}, at 56% hydrogen utilization and 47% oxygen utilization

- Electrochemical characterization (j-V curve, impedance spectroscopy)
- Change the hydrogen electrode feed to 1000 ml min^{-1} H_2 + 1000 ml min^{-1} H_2O
- Cell operation in fuel cell mode during 24 h at 1 A cm^{-2}, at 56% hydrogen utilization and 47% oxygen utilization
- Electrochemical characterization (j-V curve, impedance spectroscopy)
- Cell operation in electrolyzer mode during 300 h at 1 A cm^{-2}, at 60% steam utilization
- Electrochemical characterization (j-V curve, impedance spectroscopy)
- Cell operation in electrolyzer mode at 1 A cm^{-2}, at 60% steam utilization for undetermined time period
- Electrochemical characterization (j-V curve, impedance spectroscopy)
- Cell cooling with 4% hydrogen in N_2 at the hydrogen electrode and N_2-O_2 80-20 vol% at the oxygen electrode

3 Results

Figure 1 shows the j-V behaviour of the tested cells in electrolyzer mode, while feeding the hydrogen electrode with H_2-50%H_2O at the hydrogen electrode and the oxygen electrode with N_2-O_2 80-20 vol%. No current limiting behaviour was observed beyond 60%. Furthermore, a striking similarity in j-V behaviour between both cells with 215 µm thick electrolyte can be observed. This indicates good reproducibility of the cell performance in electrolyzer mode.

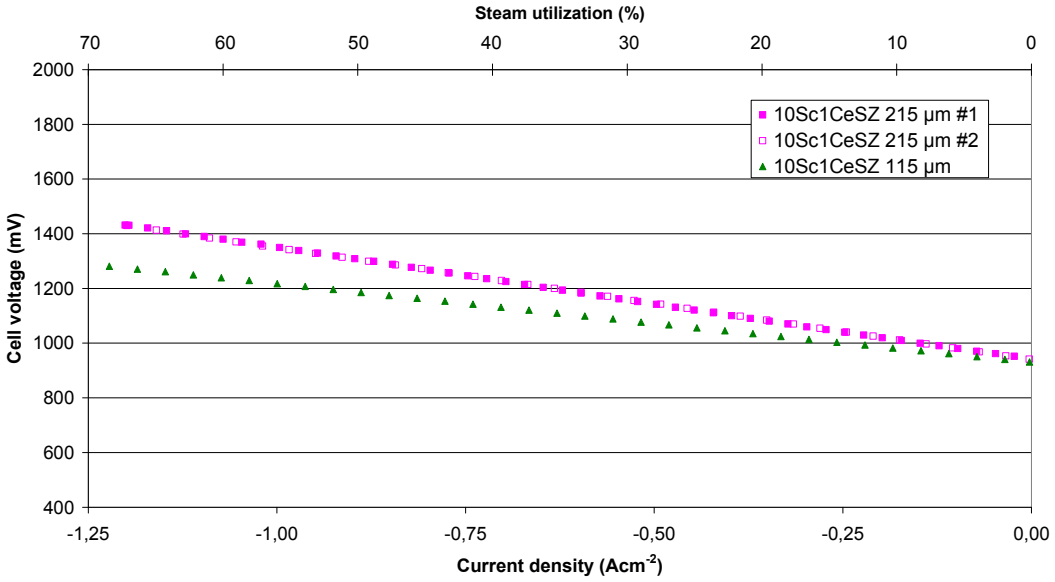

Figure 1: j-V behaviour in electrolyzer mode at 800°C, feeding H_2-H_2O 50-50 vol% to the hydrogen electrode and N_2-O_2 80-20 vol% to the oxygen electrode.

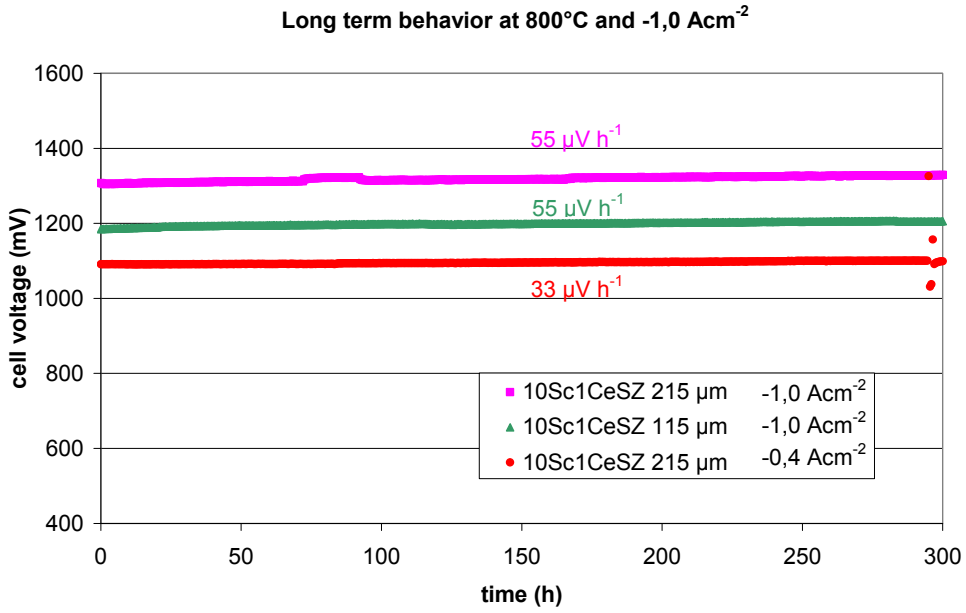

Figure 2: Long term behaviour in electrolyzer mode at 800°C, feeding H_2-H_2O 50-50 vol% to the hydrogen electrode and N_2-O_2 80-20 vol% to the oxygen electrode.

The long term behaviour of the cells in electrolyzer mode is shown in figure 2. For the cells operated at -1 Acm^{-2}, comparable degradation rates were observed. The cell that was operated at a modest current density of -0.4 Acm^{-2} exhibited a lower degradation rate.

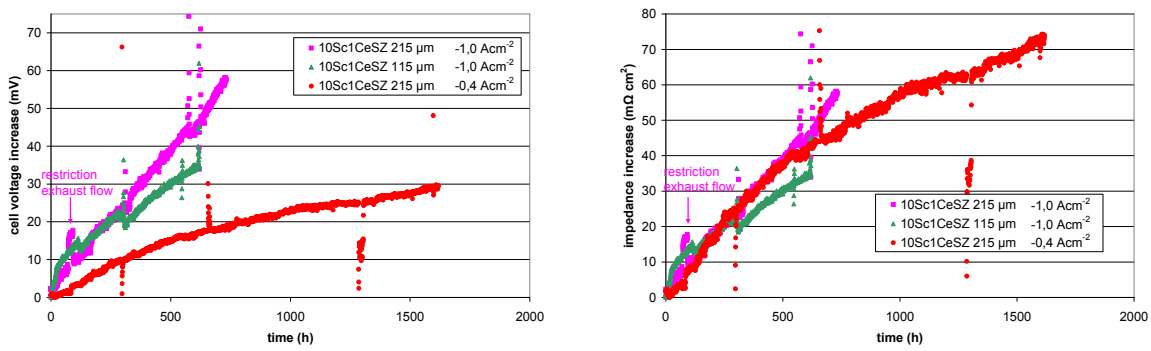

Figure 3: Long term behaviour in electrolyzer mode at 800°C, feeding H_2-H_2O 50-50 vol% to the hydrogen electrode and N_2-O_2 80-20 vol% to the oxygen electrode.

In order to get further insight in the degradation behaviour of the cells, Figure 3 was produced. At the left hand side, the voltage increase with time is shown, while at the right hand side, the increase of the internal resistance (i.e., cell voltage increase divided by operating current density) with time is shown. This makes clear that the lower degradation rate of the cell operated at the modest current density of -0.4 A cm^{-2} is related to the operating current density, not to better stability of the cell internal resistance.

Something else that can be seen in figure 3 is that the durability graphs were prone too several artefacts. First, an artefact was observed in the cell voltage of one of the cells. This

was probably caused by malfunctioning of the Peltier cooler which allowed condensed water to restrict the exhaust flow. Furthermore, it was observed that j-V measurements sometimes had a long term impact on the cell voltage. It is unlikely that this is related to temporary effects such as a temperature change induced by a change in Joule heat during the j-V measurement. More likely, the long term effect is caused by rearrangement of the electrical contact between the current collecting meshes due to thermal stresses released during the j-V measurement.

In order to deconvolute the impedance spectra that have been recorded throughout the tests, additional measurements have been carried out on the cell with 215 µm thick 10Sc1CeSZ electrolyte that was operated at -1.0 Acm^{-2}. At 800°C, impedance spectra were recorded at fixed current density as a function of the hydrogen electrode and oxygen electrode gas feeds. Furthermore, impedance spectra were recorded at 750, 700 and 650°C as a function of current density and oxygen electrode gas feed (either N_2-O_2 80-20 vol% or O_2 100 vol%). These measurements made clear that the polarization resistance exists of four different contributions, here denoted Rp1, Rp2, Rp3 and Rp4. See, for example, the impedance spectra depicted in figure 4. Polarization term Rp1 has a typical turnover frequency of between 15 kHz (650°C). Polarization term Rp2 has a turnover frequency of between 300 Hz (650°C). Polarization terms Rp1 and Rp2 were inseparable above 700°C, so separate interpretation was only possible at 650 and 700°C, whereas above 700°C only the sum of Rp1 and Rp2 was considered. Polarization resistance Rp3 had a turnover frequency of about 30 Hz (650-800°C). Polarization resistance Rp4 had a turnover frequency of 1.5 Hz (650-800°C). Besides the polarization terms Rp1 until Rp4, the impedance spectra comprised a serial resistance Rs, which is a summation of the ohmic losses existing in the cell, prominently the ionic resistance of the electrolyte. The complete equivalent circuit used during the fitting exercise is shown in figure 5. Next to the resistors mentioned, it comprised four capacitances in parallel with the polarization resistances, and at 750 and 800°C, an inductance L that was induced by the wiring between the potentiostat and the cell.

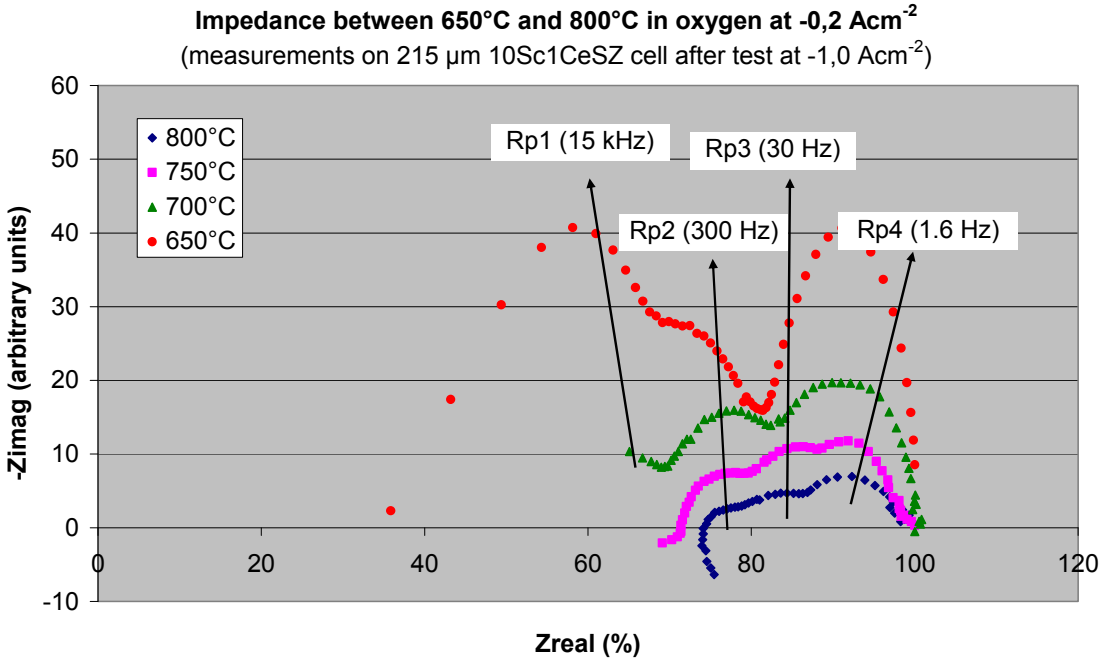

Figure 4: **Impedance spectra recorded on the cell with 215 µm thick 10Sc1CeSZ electrolyte as a function of operation temperature, under H_2-50%H_2O and N_2-O_2 80-20% gas feeds, at -0.25 A cm^{-2}.**

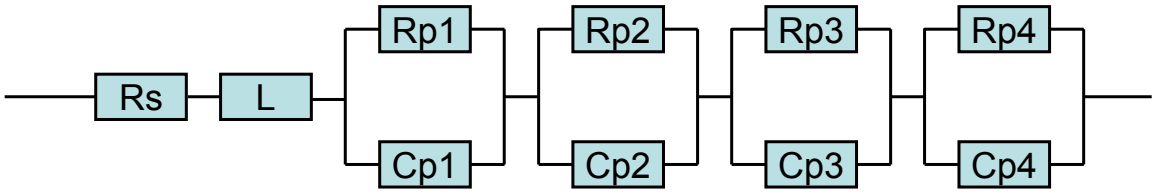

Figure 5: **Equivalent circuit used to fit the obtained impedance spectra. Below 750°C, the inductance L was visible in the impedance spectra and therefore omitted in the equivalent circuit. Above 700°C, the spectra were fitted with only three polarization repetitions.**

Figure 6 shows the values for Rs, Rp1+2, Rp3 and Rp4 for the three tested cells, obtained after approximately 300 h testing. The lower serial resistance Rs for the cell with the thinnest electrolyte is clearly the result of the lower electrolyte resistance, but not in a completely linear fashion. This indicates that Rs is not only related to the lower bulk resistance but also to other, unknown, ohmic losses. Furthermore, it can be seen that the polarization contributions were more or less comparable. Somewhat lower polarization resistance can be observed for the cell with 115 µm thick electrolyte which, in comparison with figure 3, could indicate that at the start of the test under electrolyzer conditions, the polarization resistance values were more comparable than after 300 h operation. There are however no initial impedance data available that could confirm this. Something else that can be seen from figure 5 is that both cells with 215 µm thick electrolyte have similar internal resistance. This

indicates that operation at -1.0 A cm^{-2} for 300 h has no detrimental effect on the internal resistance, compared to operation at -0.4 A cm^{-2}.

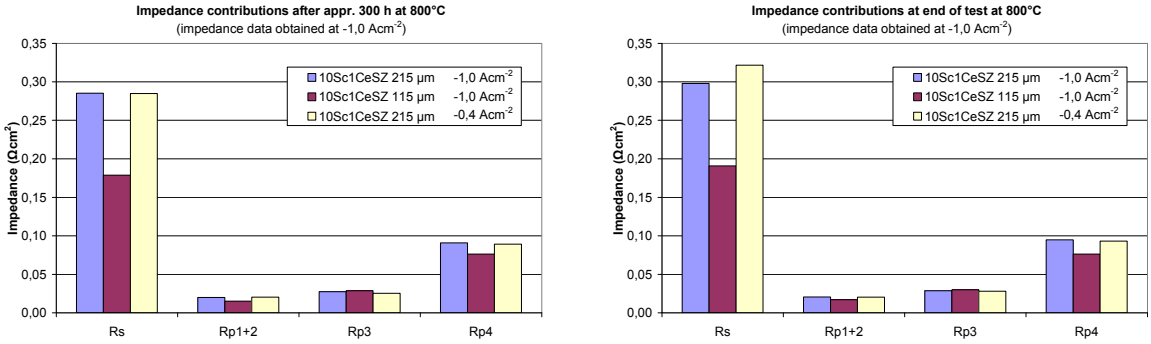

Figure 6: Impedance contributions after 300 h operation (left hand side) and at the end of the test in electrolyzer mode (right hand side).

Figure 7 shows how the resistance contributions evolved after 300 h operation under electrolyzer conditions. It makes clear that degradation is prominently related to an increase of the ohmic losses. Remarkably, the cell operated at -0.4 A cm^{-2} shows the largest increase of Rs. This could be caused by increased bulk resistivity of the electrolyte itself, but also by reduced electrochemical activity of the electrodes, which restricts the electrolyte surface area that is active in oxygen ion exchange. In order to identify the cause of the increase, it is therefore worthwhile to study the increase of the polarization resistances in more detail. For this reason, figure 8 was made, which gives the relative increase of the respective resistance contributions. This time, it can be seen that, although the polarization resistance values itself are modest, they do exhibit a considerable increase with time. It can be observed that the cells operated at -1,0 A cm^{-2} exhibit a considerably higher increase in the polarization term Rp1+2 in comparison with the cell operated at -0,4 A cm^{-2}. The other polarization terms do not show a clear dependency on electrolyte thickness or operating current density. Figure 9, that arranges the impedance contributions as a function of cell operation time, however makes clear that the polarization terms Rs, Rp3 and Rp4 rather increase with time than with operating current density. From the available data it cannot be determined whether the increase with time has a linear or a logarithmic dependency.

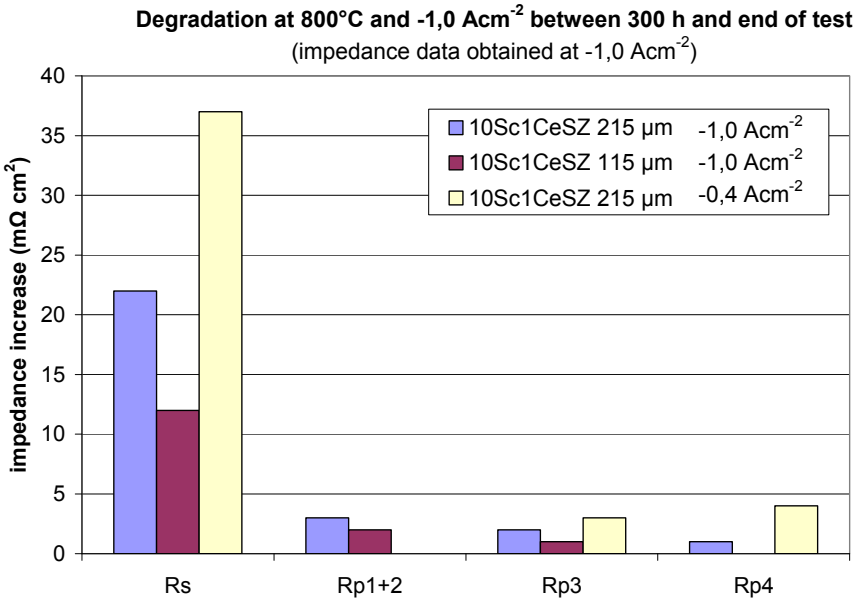

Figure 7: Impedance increase in Ωcm^2 between the first electrochemical characterization session after 300 h and the characterization session at the end of the test.

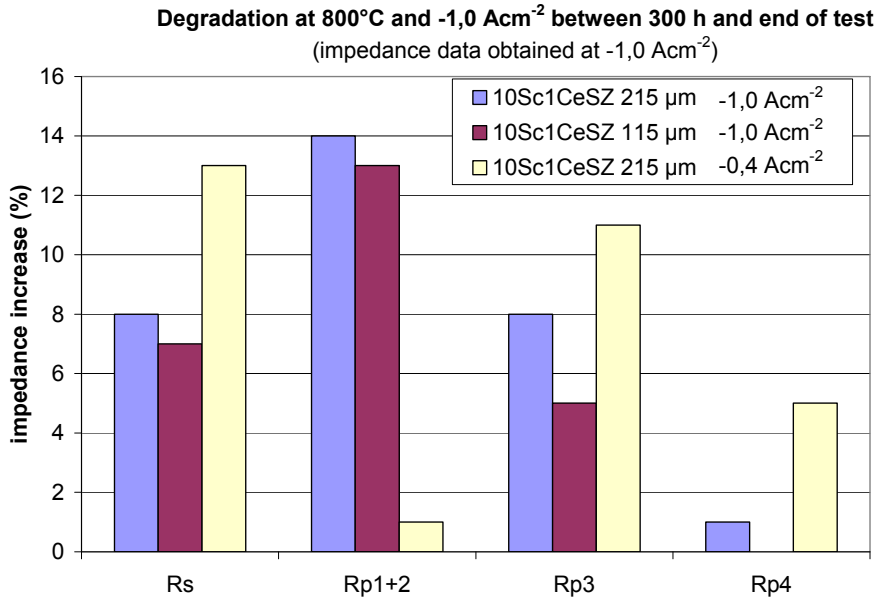

Figure 8: Impedance increase in % between the first electrochemical characterization session after 300 h and the characterization session at the end of the test.

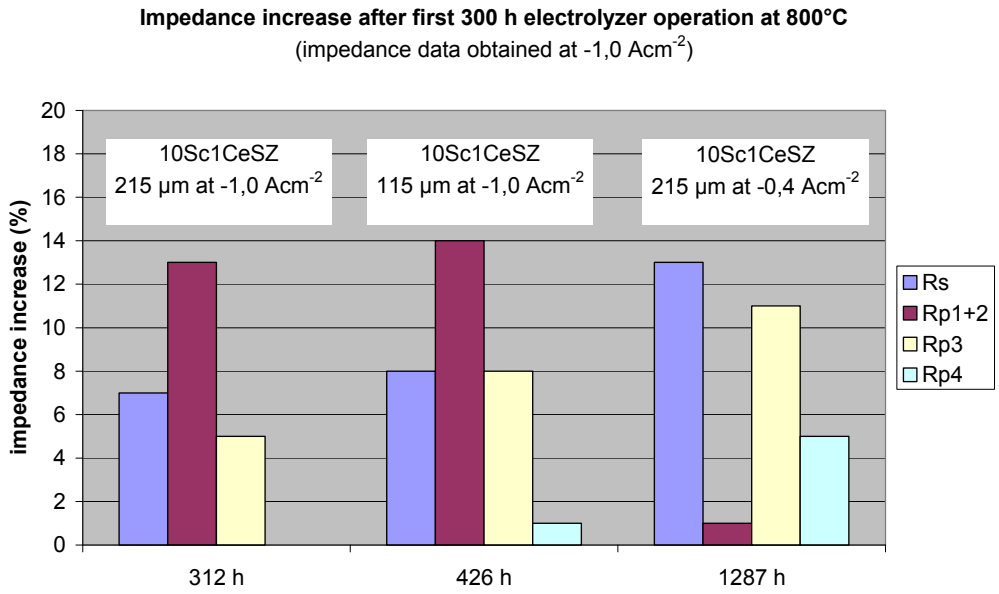

Figure 9: Impedance increase between the first electrochemical characterization session and the characterization session at the end of the test.

Figure 10 shows several graphs that have been produced in order to reveal the dependency of the polarization contributions to the oxygen electrode gas feed and the hydrogen electrode gas feed. This made clear that:

- Polarization resistance Rp4 (turnover frequency at 1.6 Hz) is dependent on both the hydrogen electrode gas feed (increasing resistance with increasing pH_2O) and the oxygen electrode gas feed (decreasing resistance with decreasing pO_2). It can be observed that Rp4 shows a hyperbolic dependency on current load in fuel cell mode and electrolyzer mode. This indicates that Rp4 is a summation of mass transport limited processes occurring at the hydrogen electrode and the oxygen electrode.
- Polarization resistance Rp3 (turnover frequency at 30 Hz) is weakly dependent on pH_2O, more prominently on the pO_2, and not dependent on current density. This indicates that Rp3 is related to a bulk rate limiting process in the oxygen electrode.
- Polarization resistance Rp2 (turnover frequency at 300 Hz) is strongly dependent on pO_2 (in particular this was observed at 650°C). This indicates that Rp2 is related to a bulk rate limiting process in the oxygen electrode.
- Polarization resistance Rp1 (turnover frequency at 15 kHz) is not dependent on the oxygen electrode gas feed. It has not been determined if Rp1 is dependent on the hydrogen electrode feed. But as the sum of Rp1 and Rp2 has been shown as function of both the pH_2O and pO_2, while Rp2 is hardly dependent on pH_2O, it is likely that Rp1 is related to a bulk rate limiting process in the hydrogen electrode.

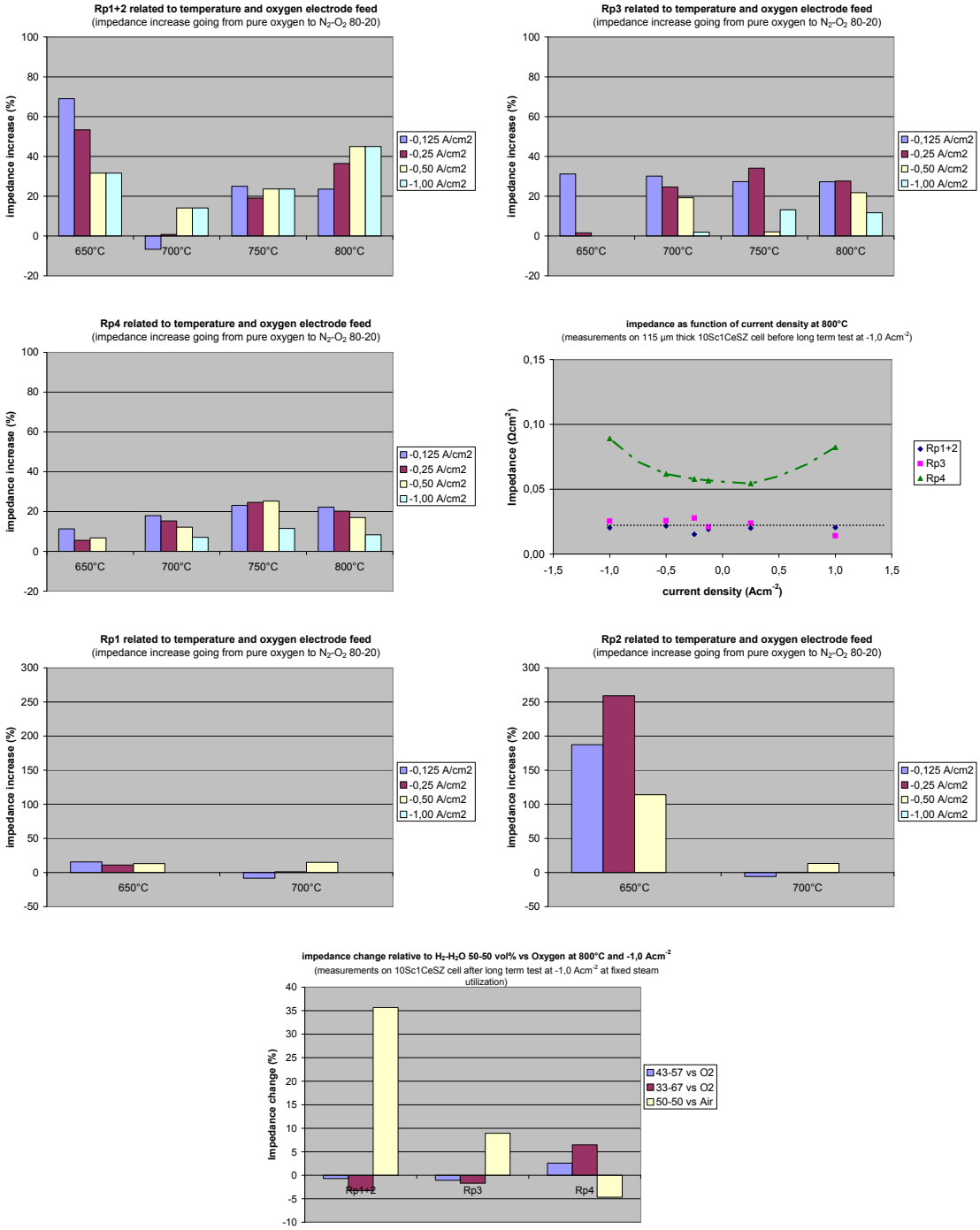

Figure 10: Polarization contributions Rp1, Rp2 (or the sum of Rp1 and Rp2), Rp3 and Rp4 as a function of temperature, operation current density, hydrogen electrode feed composition and oxygen electrode feed composition.

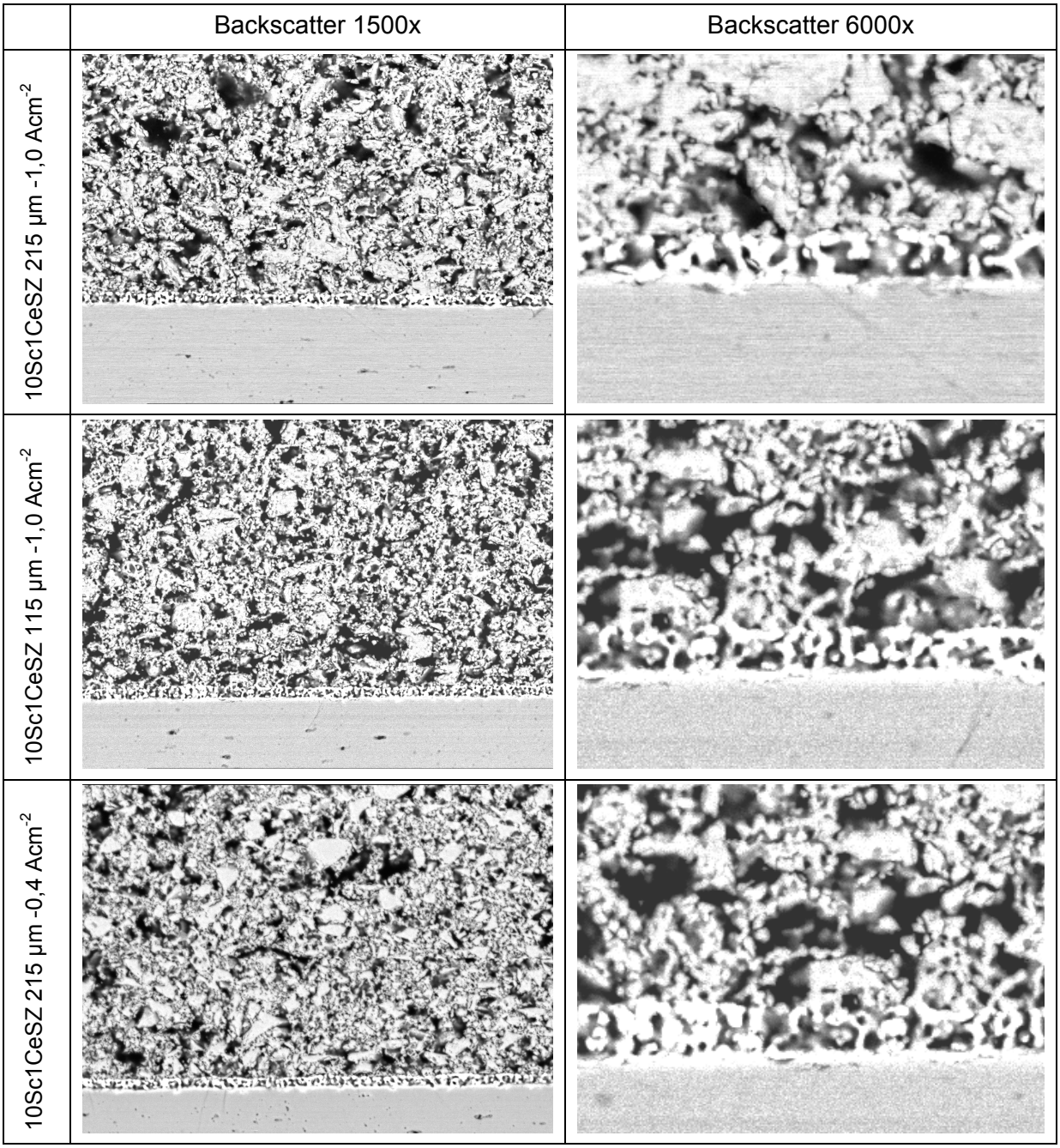

Figure 11: Scanning electron micrographs of the oxygen electrodes after testing. At the bottom of the micrographs, the 10Sc1CeSZ electrolyte can be seen. On top of the electrolyte, an approximately 5 µm thick porous YDC layer can be distinguished. Finally, on top of the YDC layer the porous, approximately 70 µm thick LSCF layer can be seen.

Figure 11 shows micrographs of the tested oxygen electrodes. The microstructures have been assessed with respect to LSCF grain size, 10Sc1CeSZ / YDC and YDC / LSCF interface adherence and thickness of the diffusion layer that has formed at the 10Sc1CeSZ / YDC interface. This revealed no significant differences that could be related to the two

observed degradation phenomena observed with impedance spectroscopy. Maybe the answer for the degradation phenomena is a more subtle one. In a previous paper from our group, it has been proposed that oxygen ion conducting perovskites such as LSCF could be prone to decreased oxygen desorption kinetics from the LSCF grains in electrolyzer mode, or decreased oxygen ion mobility in the bulk of the grains [2], but more investigation would be needed to obtain more certainty to that respect.

4 Conclusions

This paper summarizes the results that have been obtained at ECN on electrolyte supported solid oxide electrolyzer cells operated at 800°C and -1,0 Acm^{-2} current load. From long term electrochemical test under conditions similar to those aimed by the European project RelHy, the long term stability of the cells has been assessed and valuable insight in degradation phenomena at such high current load has been obtained. From impedance analysis that has been carried out throughout the tests it has become clear that the long term stability of electrolyte supported cells operated at -1.0 A cm^{-2} is related to two degradation phenomena occurring at the oxygen electrode. The first is reflected in an increase of polarization resistance at a turnover frequency of 300 Hz, which is only weakly existent at an operating current density of -0,4 A cm^{-2}, but strongly existent at -1,0 A cm^{-2}. The second degradation mechanism is reflected in an increase of polarization resistance at a turnover frequency of 30 Hz. This degradation phenomenon is not dependent on operation current density but on the electrolyzer operation time. The performed post test analyses, that focused on the microstructures, diffusion layer thicknesses and adherences between the interfaces at the oxygen electrode side of the cells, did not reveal the cause of the degradation phenomena.

Acknowledgements

This work is part of the RelHy project funded by the European Commission in the 7th Framework Program (Grant Agreement 213009).

References

[1] J.P. Ouweltjes, M.M.A. van Tuel, F.P.F. van Berkel, G. Rietveld, *Solid Oxide Electrolyzers for Efficient Hydrogen Production*, in: 10th International Symposium on Solid Oxide Fuel Cells (SOFC-X), June 2007, Nara, Japan, p. 933

[2] J.P. Ouweltjes, M. van Tuel, F. van Berkel, G. Rietveld, *Electrical Efficiency and Electrochemical Stability of Cathode Supported Electrolyzers*, in: Proceedings 9th European Solid Oxide Fuel Cell Forum, June 30 - July 3, 2009, Lucerne, Switzerland

[3] D.-S. Lee, W.S. Kim, S.H. Choi, J. Kim, H.-W. Lee, J.-H. Lee, Sol. St. Ionics 176 (2005) 33.